Alignment of heavy few-electron ions following excitation by relativistic Coulomb collisions

Andrey Surzhykov,[1,2,*] Ulrich D. Jentschura,[1,3] Thomas Stöhlker,[2,4] Alexandre Gumberidze,[4] and Stephan Fritzsche[4,†]
[1]*Max-Planck-Institut für Kernphysik, Postfach 103980, D-69029 Heidelberg, Germany*
[2]*Physikalisches Institut, Universität Heidelberg, D-69120 Heidelberg, Germany*
[3]*Institut für Theoretische Physik, Universität Heidelberg, D-69120 Heidelberg, Germany*
[4]*Gesellschaft für Schwerionenforschung (GSI), D-64291 Darmstadt, Germany*
(Received 8 October 2007; published 28 April 2008)

The Coulomb excitation of highly charged few-electron ions in relativistic collisions with protons and low-Z atoms is studied within the framework of first-order perturbation theory and the multiconfiguration Dirac-Fock method. Apart from the computation of the total excitation cross sections, a detailed theoretical analysis has been performed for the magnetic sublevel population of the residual ions. To describe this population, general expressions are derived for the alignment parameters of the excited states of the ions, taking into account the relativistic and many-electron effects. Calculations are performed for the $K \rightarrow L$ and $K \rightarrow M$ excitation of helium- and lithiumlike uranium ions and for a wide range of projectile energies. It is shown that the alignment of heavy few-electron ions is sensitive to relativistic and magnetic-interaction effects and, hence, to the collision energies of the projectiles. The theoretical predictions are discussed in the context of recent measurements on the Coulomb excitation of heliumlike uranium U^{90+} ions which were recently performed at the GSI storage ring in Darmstadt.

DOI: 10.1103/PhysRevA.77.042722 PACS number(s): 34.50.Fa, 31.15.V−, 31.30.J−

I. INTRODUCTION

Owing to recent advances in heavy-ion storage rings [1–5] and electron-beam ion traps (EBITs) [6,7], new ion-electron and ion-atom collision experiments have become possible during the last decade. In these collision experiments, attention was first paid to those processes that may lead to the formation of *excited* or *ionized* states of the projectile ions. In the high-Z domain, the deexcitation of these states then usually results in the emission of one (or several) x-ray photons until the ground state is reached. Indeed, the analysis of the "characteristic" radiation has attracted much recent interest, by both experiment and theory, since it helps to improve our understanding of the electronic structure as well as of the population dynamics of highly charged ions. For example, recent investigations of the angular distribution and linear polarization of the characteristic radiation, following the *radiative electron capture* (REC) into the excited states of high-Z, bare ions, have revealed valuable information about the multipole-mixing phenomena in heavy atomic systems [5,8–10]. In a series of experiments, moreover, the x-ray emission from the projectile ions provided insight into the *inner-shell ionization* of heavy ions at storage rings [11,12].

Among other processes, the Coulomb *excitation* of few-electron ions by collisions with electrons and atoms also leads to the formation of excited ionic states. In these ion-atom or ion-electron collision experiments, a *preferred* direction is typically defined for the overall systems, both at storage rings and at electron-beam ion traps. Obviously, such a preferred direction may result also in an *alignment* of the excited ions—that is, an unequal population of the magnetic sublevels of the ion with different moduli of the (magnetic) quantum number $|M_J|$—and subsequently in an anisotropic emission and nonzero polarization of the characteristic x-ray photons [13–15]. In the past, the angle- and polarization-resolved analysis of the characteristic radiation has been of ongoing interest owing to its importance for the diagnostics of high-temperature laboratory and astrophysical plasmas [13,14,16–20].

However, while most investigations of the Coulomb excitation in ion-atom collisions and the subsequent radiation dealt in the past with low- and medium-Z few-electron ions [21–29], there is a lack of data for the high-Z domain and relativistic ions. Only for the case of H- and He-like bismuth ions have final-state resolved data been reported [30,31]. These data were discussed in detail with fully relativistic calculations performed on the basis of first-order perturbation theory for the pure one-electron case. These findings underline that only a complete consideration of the Lienard-Wiechert potential allows the investigation of the role of the magnetic interaction in relativistic ion-atom collisions [32]. However, within the latter experiment, only total x-ray yields were studied. A first experiment on the *angular distribution* of the characteristic x-ray emission, following the Coulomb excitation of heliumlike U^{90+} projectiles in collision with N_2 target molecules, has been performed only recently at the GSI storage ring [33]. For He-like U^{90+} ions, the analysis of the measured emission pattern allowed one to obtain detailed information about the magnetic sublevel population of the $1s2p_{1/2}\ ^3P_1$ and $1s2p_{3/2}\ ^1P_1$ ionic states. Up to the present, however, no comparison between these experimental results and theoretical predictions has been done because of the lack of fully relativistic calculations for the excitation of high-Z few-electron projectiles. Therefore, a rigorous theoretical analysis for the Coulomb excitation of heavy projectiles is highly desirable, including both the relativistic and many-body effects of high-Z few-electron ions.

*surz@mpi-hd.mpg.de
†Present address: Max-Planck-Institut für Kernphysik, D-69117 Heidelberg, Germany.

In this contribution, first-order perturbation theory is applied in order to explore the alignment of high-Z few-electron ions following their Coulomb excitation in collisions with (low-Z) targets. We suppose that the alignment of the excited projectiles is determined completely by the partial cross sections for the excitation into the magnetic sublevels, leaving apart possible "cascade" effects due to the decay of some energetically high-lying levels. In Sec. II A, we shall first discuss the evaluation of the (Coulomb) excitation amplitudes and cross sections within the semiclassical approximation (SCA), in which the projectile is assumed to move with constant velocity along a straight-line trajectory. For fast collisions of heavy projectiles, this approximation is well justified and has been utilized at a number of places. In particular, here we explain how the partial excitation cross sections can be traced back always to the bound-bound transition amplitudes whose properties are discussed in Sec. II B. The computation of these amplitudes within the framework of the multiconfiguration Dirac-Fock (MCDF) method is later outlined in Sec. III and utilized in order to determine the alignment of helium- and lithiumlike uranium following the $K \to L$ and $K \to M$ excitation of a $1s$ electron. The results of our many-electron calculations are presented in Sec. IV and are discussed in the context of recent experimental data. Finally, a brief summary and outlook are given in Sec. V.

II. THEORY

A. Projectile excitation in the semiclassical picture: General formalism

Since the first-order perturbation theory has been applied very frequently in the study of heavy-ion collisions, here we restrict ourselves to a short account of the basic formulas and shall refer for all further details to the literature [4,32,34–37]. In the semiclassical picture, the projectile moves with a fixed velocity $\beta_p = v_p/c$, relative to the speed of light c, along a straight-line trajectory which is characterized by the impact parameter b. A (Coulomb) excitation or ionization of the projectile may occur in this picture due to the Lienard-Wiechert potential of the target atoms,

$$A^{\mu} = \sum_{i=1}^{N} \gamma_p \frac{\alpha Z_T}{r_i'}(1,0,0,+\beta_p), \tag{1}$$

as *seen* by the projectile electrons. In this potential, Z_T is the charge of the target nucleus, $\gamma_p = (1-\beta_p^2)^{-1/2}$ and $r_i' = [(x_i - b)^2 + y_i^2 + \gamma_p^2 (z_i - v_p t)^2]^{1/2}$ denotes the (time-dependent) distance between the target nucleus and the ith projectile electron.

Starting from the vector potential (1), we can evaluate the transition amplitudes, for both the excitation and ionization of the projectiles electrons [4]. For the case of excitation, we suppose that the ion is in the (many-electron) state $|\alpha_i J_i M_i\rangle$ *before* the excitation occurs and in the state $|\alpha_f J_f M_f\rangle$ *after* it has passed the target—i.e., that a transition occurs between two states with well-defined total angular momentum $J_{i,f}$ and its projection $M_{i,f}$ on the quantization axis. In this notation, moreover, $\alpha_{i,f}$ denote all the additional quantum numbers that are needed in order to specify the many-electron states uniquely. For the excitation $|i\rangle \to |f\rangle$, then, the amplitude in first-order perturbation theory is given in natural units ($\hbar = m_e = c = 1$) by [4,35]

$$A_{fi}(b;M_i,M_f) = i\gamma_p \alpha Z_T \int dt\, e^{i(E_f - E_i)t} \langle \alpha_f J_f M_f | \sum_{i=1}^{N} \frac{1 - \beta_p \hat{\alpha}_3(i)}{r_i'(t)} | \alpha_i J_i M_i \rangle, \tag{2}$$

where E_i and E_f denote the total energies of the projectile ion in the initial and final states, and $\hat{\alpha}_3(i) \equiv \hat{\alpha}_z(i)$ is the Dirac matrix for the ith particle. From this transition amplitude, the cross section for an excitation of the projectile, being initially in the level i, into the sublevel $|\alpha_f J_f M_f\rangle$ is obtained by integrating over all the impact parameters,

$$\sigma(\alpha_f J_f M_f) = \frac{2\pi}{2J_i + 1} \sum_{M_i} \int_0^{\infty} db\, b |A_{fi}(b;M_i,M_f)|^2, \tag{3}$$

and by performing the average over the initial magnetic sublevels M_i.

Equation (3) together with the transition amplitude (2) can be employed to calculate the partial excitation cross sections and, hence, the alignment of the projectile ions after an excitation has occurred. For practical use, however, it is often more convenient to reformulate these expressions in momentum space. Performing the Fourier transformation from the coordinate to momentum space and making use of some simple algebra [32,35,37], one is able to evaluate the integrals over the time t and the impact parameter b *analytically* and to reexpress the partial excitation cross section (3) in the form

$$\sigma(\alpha_f J_f M_f) = 2\pi \left(\frac{8\pi Z_T \alpha}{\beta_p} \right)^2 \frac{1}{2J_i + 1} \times \sum_{M_i} \int_{q_0}^{\infty} \frac{q dq}{[q^2 - (q_0 \beta_p)^2]^2} |\mathcal{M}_{fi}(\boldsymbol{s};M_i,M_f)|^2, \tag{4}$$

with the transition amplitude

$$\mathcal{M}_{fi}(\boldsymbol{s};M_i,M_f) = \sum_{LM} i^L Y_{LM}^*(\arccos(q_0/q),0) \langle \alpha_f J_f M_f | \sum_{i=1}^{N} [1 - \beta_p \hat{\alpha}_3(i)] j_L(q r_i) Y_{LM}(\hat{n}_i) | \alpha_i J_i M_i \rangle, \tag{5}$$

which can easily be expanded into a series of multipole components. Instead of the (integration over the) impact parameter b, Eq. (4) now contains an integration over the momentum transfer q, starting from the minimum transfer $q_0=(E_f-E_i)/v_p$ that is necessary in order to excite the ion from the initial level $|\alpha_i J_i\rangle$ to the level $|\alpha_f J_f\rangle$.

Equations (4) and (5) describe the Coulomb excitation of an ion between states of well-defined symmetry. Before we continue to simplify this transition amplitude and partial cross sections, let us note here that Eqs. (4) and (5) neglect the interaction of the projectile electron with the electrons of the target atom. In the theory of ion-atom collisions, however, the influence of the target electrons onto the projectile transitions between the bound states is known to be twofold [38–40]: Apart from (i) the presence of the target electrons, which result in a partial *screening* of the (nuclear) target potential and, hence, a slight reduction of the excitation cross sections, (ii) the *same* electrons may "excite" also the projectile electrons due to Coulomb collisions, an effect which is known as *antiscreening* from the literature [4,5]. Both these effects can be quite sizable for the total cross sections, but are of less importance for the alignment of the excited ionic states. In the present work, therefore, we shall neglect these effects and concentrate instead on the electron-electron interactions that appear in the heavy, few-electron projectiles themselves.

B. Evaluation of transition amplitudes

Equation (5) displays the matrix element for the excitation of a projectile ion, assuming a representation of the retarded potential in *momentum* space. In practice, the great advantage of this expression is that the time dependence, which was contained originally in the phase and denominator of the amplitude (2), is now replaced by the dependence on the momentum variable q. This replacement enables us to make use of Racah's algebra in simplifying the excitation cross sections. To this end, let us first apply the Wigner-Eckart theorem to the second line of Eq. (5) and to rewrite the *multipole* matrix elements in the form

$$\begin{aligned}\langle \alpha_f J_f M_f | \sum_{i=1}^{N} (1-\beta_p \hat{\alpha}_3(i)) j_L(qr_i) Y_{LM}(\hat{n}_i) | \alpha_i J_i M_i \rangle &= \langle \alpha_f J_f M_f | \sum_{i=1}^{N} j_L(qr_i) Y_{LM}(\hat{n}_i) | \alpha_i J_i M_i \rangle \\ &\quad - \beta_p \langle \alpha_f J_f M_f | \sum_{i=1}^{N} \hat{\alpha}_3(i) j_L(qr_i) Y_{LM}(\hat{n}_i) | \alpha_i J_i M_i \rangle \\ &= \frac{1}{\sqrt{2J_f+1}} \langle J_i M_i LM | J_f M_f \rangle \langle \alpha_f J_f || \sum_{i=1}^{N} j_L(qr_i) Y_L(\hat{n}_i) || \alpha_i J_i \rangle \\ &\quad - \beta_p \sum_{t=L-1}^{L+1} \frac{1}{\sqrt{2J_f+1}} \langle LM10 | tM \rangle \langle J_i M_i tM | J_f M_f \rangle \\ &\quad \times \langle \alpha_f J_f || \sum_{i=1}^{N} j_L(qr_i) \hat{\boldsymbol{\alpha}}(i) \cdot \boldsymbol{T}_{tL}(\hat{n}_i) || \alpha_i J_i \rangle, \end{aligned} \tag{6}$$

where $\boldsymbol{T}^M_{tL}(\hat{n})=\Sigma_{m\mu}\langle Lm1\mu|tM\rangle Y_{Lm}(\hat{n})\boldsymbol{e}_\mu$ is the standard vector spherical harmonic of total rank t [15,41]. Inserting this expression into Eq. (5), we obtain for the excitation amplitude

$$\begin{aligned}\mathcal{M}_{fi}(\boldsymbol{s};M_i,M_f) &= \sum_t \frac{1}{\sqrt{2J_f+1}} \langle J_i M_i tM_f - M_i | J_f M_f \rangle \\ &\quad \times \sum_L i^L Y^*_{LM_f-M_i}(\arccos(q_0/q),0) \\ &\quad \times \langle \alpha_f J_f || H_{tL}(q) || \alpha_i J_i \rangle, \end{aligned} \tag{7}$$

if we here define the "effective" reduced matrix element as

$$\begin{aligned}\langle \alpha_f J_f || H_{tL}(q) || \alpha_i J_i \rangle &= \delta_{tL} \langle \alpha_f J_f || \sum_{i=1}^{N} j_L(qr_i) Y_L(\hat{n}_i) || \alpha_i J_i \rangle \\ &\quad - \beta_p \langle LM10 | tM \rangle \\ &\quad \times \langle \alpha_f J_f || \sum_{i=1}^{N} j_L(qr_i) \hat{\boldsymbol{\alpha}}(i) \cdot \boldsymbol{T}_{tL}(\hat{n}_i) || \alpha_i J_i \rangle. \end{aligned} \tag{8}$$

Apparently, this effective matrix element combines two kinds of reduced matrix elements with the (many-body) transition operator $\Sigma_{i=1}^N j_L(qr_i)Y_L(\hat{n}_i)$ of rank L and $\Sigma_{i=1}^N j_L(qr_i)\hat{\boldsymbol{\alpha}}(i)\cdot\boldsymbol{T}_{tL}(\hat{n}_i)$ of rank t, respectively. In fact, these reduced matrix elements form the building blocks that are

needed in order to represent and to explore the properties of the projectile excitation. An efficient evaluation of these matrix elements for few-electron heavy ions will be briefly discussed below in Sec. III.

C. Alignment of the excited ionic states

The partial cross sections (4), together with the many-particle transition amplitudes (7), describe the excitation of the projectile into a given magnetic sublevel of the ion. If the cascade feeding from higher-lying levels is neglected, these cross sections also define the *relative population* of the sublevels $|\alpha_f J_f M_f\rangle$, following the collision with the target nucleus. For a fixed and well-defined direction of the ion beam, this—residual—population usually deviates from a statistical distribution. In general, (an ensemble of) excited ions is said to be *aligned* if all sublevels with the same modulus of the magnetic quantum number $|M_f|$ are equally populated, but levels with different moduli are not. Usually, the alignment of the residual ions is described in terms of one (or several) parameters $\mathcal{A}_k(\alpha_f J_f)$ which are related to the partial cross sections $\sigma(M_f)$ as [15,42,43]

$$\mathcal{A}_k(\alpha_f J_f) = \frac{\sqrt{2J_f+1}}{\sigma(\alpha_f J_f)} \sum_{M_f} (-1)^{J_f - M_f} \langle J_f M_f J_f - M_f | k 0 \rangle \sigma(\alpha_f J_f M_f) \tag{9}$$

and where

$$\sigma(\alpha_f J_f) = \sum_{M_f} \sigma(\alpha_f J_f M_f) \tag{10}$$

denotes the *total* excitation cross section. Moreover, as seen from this relation and the symmetry properties of the Clebsch-Gordan coefficients, the alignment parameters $\mathcal{A}_k(\alpha_f J_f)$ obey two important properties: They can be *nonzero* only if k is even and if the condition $k \leq 2J_f$ is satisfied [42]. For the projectile excitation to any level with $J_f = 1$ or 3/2, therefore, the alignment of the residual ion is characterized by the single parameter

$$\mathcal{A}_2(\alpha_f \ J_f = 1) = \sqrt{2} \frac{\sigma(\alpha_f \ J_f = 1 \ M_f = \pm 1) - \sigma(\alpha_f \ J_f = 1 \ M_f = 0)}{\sigma(\alpha_f \ J_f = 1 \ M_f = 0) + 2\sigma(\alpha_f \ J_f = 1 \ M_f = \pm 1)} \tag{11}$$

or

$$\mathcal{A}_2\left(\alpha_f \ J_f = \tfrac{3}{2}\right) = \frac{\sigma\left(\alpha_f \ J_f = \frac{3}{2} \ M_f = \pm \frac{3}{2}\right) - \sigma\left(\alpha_f \ J_f = \frac{3}{2} \ M_f = \pm \frac{1}{2}\right)}{\sigma\left(\alpha_f \ J_f = \frac{3}{2} \ M_f = \pm \frac{1}{2}\right) + \sigma\left(\alpha_f \ J_f = \frac{3}{2} \ M_f = \pm \frac{3}{2}\right)}, \tag{12}$$

while two parameters $\mathcal{A}_2$ and $\mathcal{A}_4$ are required to describe the relative population (of the magnetic sublevels) for all levels with $J_f = 2$ or $J_f = 5/2$, respectively. Another property of the alignment parameters $\mathcal{A}_k(\alpha_f J_f)$ which follows immediately from Eqs. (4) and (9) is that—within the first-order theory—these parameters do not depend on the charge of the target nucleus Z_T. The numerical results presented in Sec. IV, therefore, describe the projectile alignment following collisions with both the protons and low-Z target atoms.

III. COMPUTATIONS

For any further analysis of the partial excitation cross sections or alignment of the excited projectiles, we need to compute the reduced matrix elements $\langle \alpha_f J_f || H_{tL}(q) || \alpha_i J_i \rangle$ as seen from Eqs. (6)–(9) above. Matrix elements of this or similar type occur frequently in atomic structure and have therefore been implemented in a number of codes [44–48]. In the present calculations below, we applied the MCDF wave functions from the GRASP92 program [49] and adopted, in addition, the RATIP code [50] in order to obtain all the cross sections and alignment parameters. In the MCDF method, an atomic (ionic) state with angular momentum J and parity P is approximated by a linear combination of (so-called) configuration state functions (CSFs) of the same symmetry:

$$\psi_\alpha(PJM) = \sum_{r=1}^{n_c} c_r(\alpha) | \gamma_r PJM \rangle. \tag{13}$$

In this ansatz, n_c is the number of CSFs and $\{c_r(\alpha)\}$ denotes the representation of the atomic state in this basis. As usual, the CSFs are antisymmetrized products of a common set of orthonormal orbitals and are optimized, together with the radial orbital functions, on the basis of the Dirac-Coulomb Hamiltonian. For high-Z few-electron ions, moreover, it is typically sufficient to generate the initial and final states together—i.e., by using a common set of radial orbitals. Further relativistic contributions due to the Breit interaction were added later by diagonalizing the Dirac-Coulomb-Breit Hamiltonian matrix, while the incorporation of radiative corrections are beyond the scope of the present work. These corrections are negligible at the present accuracy of angular resolved measurement on the capture or excitation of high-Z ions at storage rings [48].

IV. RESULTS AND DISCUSSION

As already mentioned, measurements of the excitation of high-Z few-electron projectiles at storage rings are no longer impractical today. For the K-shell excitation of heliumlike uranium ions U^{90+}, for example, first experiments have been performed recently at the GSI facility in Darmstadt [33]. In the experiments, special attention has been paid to the magnetic sublevel population of the $1s2p_{1/2}$ and $1s2p_{3/2}$ states as was deduced from the angular distributions of the subsequent $K\ \alpha_2$ and $K\ \alpha_1$ decay, correspondingly. In order to provide a theoretical support for these measurements as well as to get deeper insight into the many-body aspects of the heliumlike system studied, below we apply Eqs. (6)–(10) for analysis of the $K \rightarrow L$ excitation of uranium U^{90+} ions.

If the *single*-electron excitation appears in the collision of the heliumlike projectile with target atom (or molecule), we find the residual ion in one of the $1snlj\ ^{1,3}L_J$ excited states. For the particular case of excitation to the L shell, six (excited) states may be populated and give later a contribution

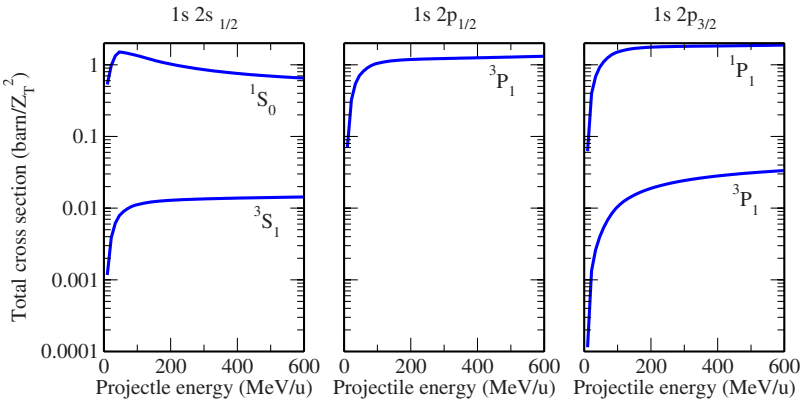

FIG. 1. (Color online) Total cross sections for the K-shell excitation of the heliumlike uranium ions U^{90+} to the different L subshells.

to the subsequent radiative decay. As seen from Fig. 1, however, the $K \rightarrow L$ excitation of heliumlike uranium ions results in an almost selective population of the $1s2s\ ^1S_0$, $1s2p_{1/2}\ ^3P_1$, and $1s2p_{3/2}\ ^1P_1$ ionic states as it was discussed early in Ref. [51]. The total cross sections (10) for these states are at least 50 times larger than the population cross sections for the other levels. Such a selective population leads to the fact that only $1s2p_{3/2}\ ^1P_1$ and $1s2p_{1/2}\ ^3P_1$ states contribute to the characteristic $K\ \alpha_1$ and $K\ \alpha_2$ lines, correspondingly. The excitation to the $1s2s\ ^1S_0$ level does not produce $K\ \alpha_2$ photons since this level decays through the two-photon $2E1$ emission.

As seen from Fig. 1 and discussion above, any analysis of the angular and polarization properties of the $K\ \alpha_{1,2}$ photons can be traced back to the magnetic sublevel population of the $1s2p_{3/2}\ ^1P_1$ and $1s2p_{1/2}\ ^3P_1$ states. For both states, this population can be described by the single alignment parameter $\mathcal{A}_2$. In the present work, we have applied Eqs. (6)–(10) together with the multiconfiguration Dirac-Fock approach in order to investigate the energy dependence of this parameter for the excitation of heliumlike uranium U^{90+} ions. One can see from Fig. 2 that alignment $\mathcal{A}_2$ of the $^3P_1$ as well as $^1P_1$ state is large and negative for low energy collisions with $T_p \leq 100$ MeV/u. This refers to a predominant population of the $M_f=0$ magnetic substate [cf. Eq. (11)] and therefore to an alignment which could be characterized as perpendicular to the beam direction. In fact, such an interpretation is consistent with a classical picture, in which the orbital angular momentum transferred in a collision is found perpendicular to the collision direction and, hence, the $K \rightarrow L$ excitation is governed mainly by the transition with $M_f=M_i=0$. For the higher collision energies, however, the classical picture is not valid anymore due to the increasing role of relativistic and magnetic effects. These effects result in a strong population of the magnetic sublevels with $M_f= \pm 1$ and subsequently in positive values of the parameter $\mathcal{A}_2$. For the projectile energy $T_p=600$ MeV/u, for instance, this parameter is as large as +0.45 and +0.27 for the $^3P_1$ and $^1P_1$ cases, indicating a—more than 65%—population of $M_f= \pm 1$ substates.

Besides analyzing the magnetic sublevel population of the $1s2p_{1/2}\ ^3P_1$ and $1s2p_{3/2}\ ^1P_1$ states for the *relatively* slow ($T_p<100$ MeV/u) and fast ($T_p>400$ MeV/u) uranium ions, it is interesting to consider the alignment parameters $\mathcal{A}_2$ at the intermediate energies of $150<T_p<400$ MeV/u—i.e., for the energy region which is available in the collisions experiments at GSI storage ring. In this region, parameters $\mathcal{A}_2(^3P_1)$ and $\mathcal{A}_2(^1P_1)$ become rather small and even vanish at energies $T_p=165$ MeV/u and $T_p=324$ MeV/u, resulting, thus, in an almost *isotropic* angular distribution of thesubsequent $K\ \alpha_2$ and $K\ \alpha_1$ lines, correspondingly. Moreover, between these two energies, the parameters $\mathcal{A}_2(^3P_1)$ and $\mathcal{A}_2(^1P_1)$ have opposite signs, indicating qualitatively different angular behavior of the characteristic photons. That is, while the subsequent $K\ \alpha_1$ radiation has maximum at the

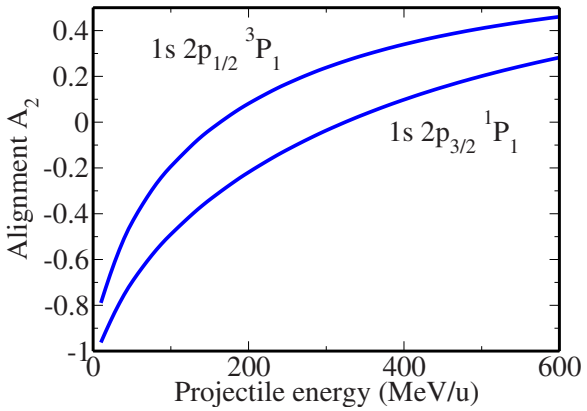

FIG. 2. (Color online) Alignment parameters $\mathcal{A}_2$ of the $1s2p_{1/2}\ ^3P_1$ and $1s2p_{3/2}\ ^1P_1$ states of heliumlike uranium U^{90+} following K-shell excitation.

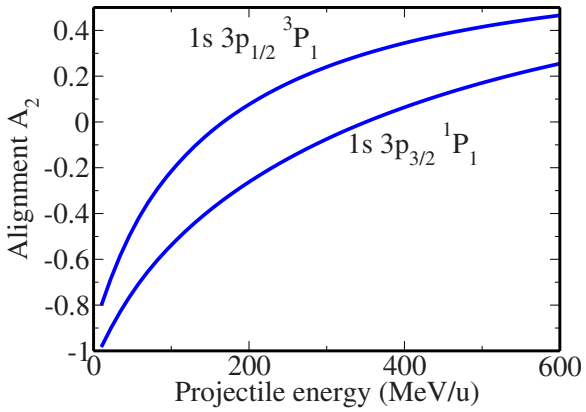

FIG. 3. (Color online) Alignment parameters $\mathcal{A}_2$ of the $1s3p_{1/2}\ ^3P_1$ and $1s3p_{3/2}\ ^1P_1$ states of heliumlike uranium U^{90+} following K-shell excitation.

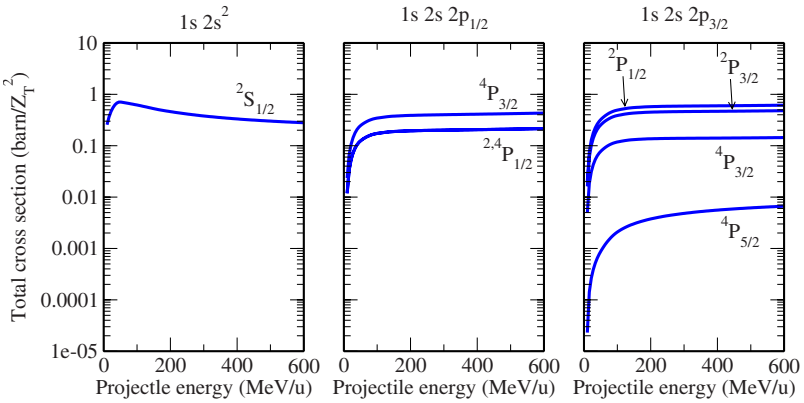

FIG. 4. (Color online) Total cross sections for the *K*-shell excitation of the lithiumlike uranium ions U^{89+} to the different $1s2s2p_{1/2,3/2}$ levels.

emission angle $\theta=90°$, the *K* α_2 angular distribution should be minimal in this direction. Such a behavior has recently been observed experimentally [52] and now is confirmed by our calculations.

Until now we have discussed Coulomb excitation of the heliumlike uranium U^{90+} ions to the different *L* subshells. In the relativistic collisions of the uranium projectiles with the target atoms (molecules), however, *M*-shell excitation is also possible and leads to a formation of *ten* $1s3lj\ ^{1,3}L_J$ levels. Again, only few of these levels will be populated strongly enough to give (significant) contribution to the subsequent radiative decay. From our calculations, based on Eq. (10), we found that the Coulomb excitation proceeds nearly exclusively to the $1s3p_{1/2}\ ^3P_1$, $1s3p_{3/2}\ ^1P_1$ and $1s3s_{1/2}\ ^1S_0$ states. Since the $3\ ^1S_0$ state cannot be aligned, we carry our alignment analysis for two *P* states. Parameters $\mathcal{A}_2$ for these states are displayed in Fig. 3 as a function of projectile energy T_p. Similar to the *L*-shell excitation, these parameters are negative for slow ions, but become large and positive for high collision energies of $T_p > 400$ MeV/u. Such a similarity can be explained by the fact that pairs of parameters $\mathcal{A}_2(2^3P_1)$ and $\mathcal{A}_2(3\ ^3P_1)$ as well as $\mathcal{A}_2(2\ ^1P_1)$ and $\mathcal{A}_2(3\ ^1P_1)$ describe the alignment of the states with the same symmetry and just differ (apart from rather weak configuration interaction terms) in the radial integrals which are used for computation of the reduced matrix elements (8).

In the discussion above, we have restricted ourselves to the excitation of the heliumlike uranium U^{90+} projectiles for which a number of studies have been performed at the GSI storage ring [33,52]. Apart from the two-electron species, most recent attention has been paid to *lithiumlike* uranium U^{89+} ions. For these ions, detailed analysis of the characteristic x-ray emission following relativistic collisions with molecular N_2 target has been carried out and has revealed important information about inner-shell ionization as well as inner- and intrashell Coulomb excitation processes [11]. In the present work, therefore, we would like to investigate the magnetic sublevel population of the lithiumlike ions following the inner-shell excitation. Such a process results in a formation of *eight* $1s2s2lj\ ^{1,3}L_J$ levels which may later decay either by emitting a characteristic x-ray or by emitting Auger electrons. Since for high-*Z* ions the autoionization is less preferable, in the present work we restrict ourselves to the discussion of the radiative decay channels. Similar to the case of the heliumlike ions, a detailed analysis of the total excitation cross sections has been performed in order to identify the lithiumlike levels which may (significantly) contribute to the anisotropy of the subsequent projectile emission. Two of such states $1s2s2p_{1/2}\ ^4P_{3/2}$ and $1s2s2p_{3/2}\ ^2P_{3/2}$ have been found from our MCDF calculations (cf. Fig. 4). Alignment parameters $\mathcal{A}_2$ for both states are displayed in Fig. 5. Again, a strong energy dependence of the alignment parameters can be seen from this figure. Moreover, similar to the heliumlike ions, negative alignment arises due to the inner-shell excitation at low projectile energies, while the relativistic and magnetic interaction effects which become stronger at high T_p lead to a predominant population of the $M_f = \pm 3/2$ substates and, hence, to the positive values of $\mathcal{A}_2$ [cf. Eq. (12)].

V. SUMMARY AND OUTLOOK

In conclusion, the Coulomb excitation of few-electron heavy ions in relativistic collisions with low-*Z* target atoms (or protons) has been studied within the framework of the first-order perturbation theory and combined with multiconfiguration Dirac-Fock computations. Special emphasis was placed on the magnetic sublevel population of the residual ions as described by set of the alignment parameters $\mathcal{A}_k$. For these parameters, general expressions have been derived which neither depend on the number of electrons nor on the shell structure of the ions under consideration. By making

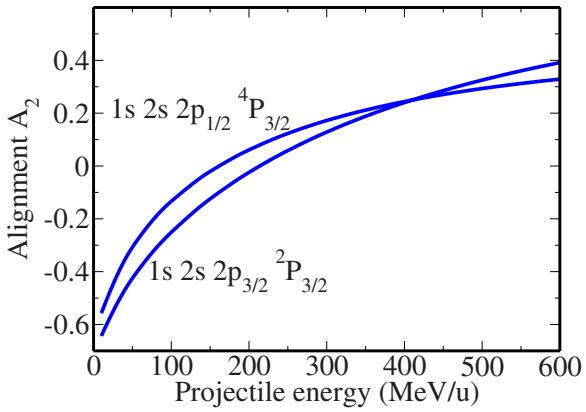

FIG. 5. (Color online) Alignment parameters $\mathcal{A}_2$ of the $1s2s2p_{1/2}\ ^4P_{3/2}$ and $1s2s2p_{3/2}\ ^2P_{3/2}$ states of lithiumlike uranium U^{89+} following *K*-shell excitation.

use of our general formalism, detailed computations were carried out for the $K \rightarrow L$ and $K \rightarrow M$ excitation of heliumlike U^{90+} and lithiumlike U^{89+} uranium projectiles. From these calculations, we found a strong dependence of the magnetic sublevel population of the residual ions on the collision energy. In particular, for relatively low projectile energies Coulomb excitation leads to a predominant population of the magnetic sublevels with minimal magnetic quantum number ($M_f=0$ for $J_f=1$ and $M_f=1/2$ for $J_f=3/2$) and, hence, to negative values of the alignment parameters; the result which can be understood within the classical, nonrelativistic picture. In contrast, the role of relativistic and magnetic interaction effects dramatically increases for higher energies of $T_p > 400$ MeV/u, resulting in significant population of the $|M_f|=J_f$ states and in large positive values of alignment. Moreover, we found the region of "intermediate" collision energies where the alignment of both the heliumlike and lithiumlike excited ions vanishes, indicating, thus, the isotropic behavior of the subsequent x-ray emission. Our alignment studies will help to understand the angular and polarization properties of the subsequent x-ray emission from high-Z few-electron projectiles which nowadays attracts much experimental interest.

The first-order perturbation approach, used in our present calculations, is appropriate for the analysis of modern collision experiments at storage rings involving heavy projectiles and light targets. If, however, the nuclear charge of the target atom Z_T increases, the interaction between the projectile electron and the atomic nucleus may become so strong that the first-order theory is not valid anymore [40]. Therefore, for an accurate treatment of the alignment of heavy ions excited in collisions with medium-Z or even high-Z targets our present theory has to be extended to take into account higher-order effects in electron-nucleus interaction. Investigations along these lines are currently under way and will support the experimental research which are likely to be carried out in the future at the GSI storage ring.

ACKNOWLEDGMENTS

U.D.J. acknowledges support by the Deutsche Forschungsgemeinschaft (Heisenberg program). S.F. acknowledges support by the BMBF and the GSI under Project No. KS-FRT. A.S. acknowledges support form the Helmholtz Gemeinschaft (Nachwuchsgruppe VH–NG–421).

[1] Th. Stöhlker, Phys. Scr. **T80**, 165 (1999).
[2] Th. Stöhlker, T. Beier, H. F. Beyer, F. Bosch, A. Brauning-Demian, A. Gumberidze, S. Hagmann, C. Kozhuharov, T. Kuhl, D. Liesen, R. Mann, P. H. Mokler, W. Quint, R. Schuch, and A. Warczak, Nucl. Instrum. Methods Phys. Res. B **235**, 494 (2005).
[3] S. Fritzsche, P. Indelicato, and Th. Stöhlker, J. Phys. B **38**, S707 (2005).
[4] J. Eichler and W. Meyerhof, *Relativistic Atomic Collisions* (Academic Press, San Diego, 1995).
[5] J. Eichler, *Lectures on Ion-Atom Collisions: From Nonrelativsitic to Relativistic Velocities* (Elsevier, Amsterdam, 2005).
[6] R. E. Marrs, P. Beiersdorfer, and D. Schneider, Phys. Today **47** (10), 27 (1994).
[7] P. Beiersdorfer, B. Beck, J. A. Becker, J. K. Lepson, and K. J. Reed, in *X-ray and Inner-Shell Processes*, edited by A. Bianconi, A. Marcelli, and N. L. Saini, AIP Conf. Proc. No. 652 (AIP, Melville, NY, 2003), p. 131.
[8] A. Surzhykov, S. Fritzsche, A. Gumberidze, and Th. Stöhlker, Phys. Rev. Lett. **88**, 153001 (2002).
[9] A. Surzhykov, S. Fritzsche, and Th. Stöhlker, Hyperfine Interact. **146-147**, 35 (2003).
[10] J. Eichler and Th. Stöhlker, Phys. Rep. **439**, 1 (2007).
[11] J. Rzadkiewicz, Th. Stöhlker, D. Banaś, H. F. Beyer, F. Bosch, C. Brandau, C. Z. Dong, S. Fritzsche, A. Gojska, A. Gumberidze, S. Hagmann, D. C. Ionescu, C. Kozhuharov, T. Nandi, R. Reuschl, D. Sierpowski, U. Spillmann, A. Surzhykov, S. Tashenov, M. Trassinelli, and S. Trotsenko, Phys. Rev. A **74**, 012511 (2006).
[12] S. Trotsenko, Th. Stöhlker, D. Banas, C. Z. Dong, S. Fritzsche, A. Gumberidze, S. Hagmann, S. Hess, P. Indelicato, C. Kozhuharov, M. Nofal, R. Reuschl, J. Rzadkiewicz, U. Spillmann, A. Surzhykov, M. Trassinelli, and G. Weber, J. Phys.: Conf. Ser. **58**, 141 (2007).
[13] M. K. Inal and J. Dubau, J. Phys. B **20**, 4221 (1987).
[14] K. J. Reed and M. H. Chen, Phys. Rev. A **48**, 3644 (1993).
[15] V. V. Balashov, A. N. Grum-Grzhimailo, and N. M. Kabachnik, *Polarization and Correlation Phenomena in Atomic Collisions* (Kluwer Academic, New York, 2000).
[16] H. L. Zhang, D. H. Sampson, and R. E. H. Clark, Phys. Rev. A **41**, 198 (1990).
[17] P. Beiersdorfer, G. Brown, S. Utter, P. Neill, K. J. Reed, A. J. Smith, and R. S. Thoe, Phys. Rev. A **60**, 4156 (1999).
[18] D. L. Robbins, A. Ya. Faenov, T. A. Pikuz, H. Chen, P. Beiersdorfer, M. J. May, J. Dunn, K. J. Reed, and A. J. Smith, Phys. Rev. A **70**, 022715 (2004).
[19] D. L. Robbins, P. Beiersdorfer, A. Ya. Faenov, T. A. Pikuz, D. B. Thorn, H. Chen, K. J. Reed, A. J. Smith, K. R. Boyce, G. V. Brown, R. L. Kelley, C. A. Kilbourne, and F. S. Porter, Phys. Rev. A **74**, 022713 (2006).
[20] G. V. Brown, P. Beiersdorfer, H. Chen, J. H. Scofield, K. R. Boyce, R. L. Kelley, C. A. Kilbourne, F. S. Porter, M. F. Gu, S. M. Kahn, and A. E. Szymkowiak, Phys. Rev. Lett. **96**, 253201 (2006).
[21] D. Detleffsen, M. Anton, A. Werner, and K. H. Schartner, J. Phys. B **27**, 4195 (1994).
[22] K. Reymann, K. H. Schartner, B. Sommer, and E. Träbert, Phys. Rev. A **38**, 2290 (1988).
[23] M. Anton, D. Detleffsen, K. H. Schartner, and A. Werner, J. Phys. B **26**, 2005 (1993).
[24] N. Stolterfoht, J. Electron Spectrosc. Relat. Phenom. **67**, 309 (1993).
[25] N. Stolterfoht, A. Mattis, D. Schneider, G. Schiwietz, B. Skogvall, B. Sulik, and S. Ricz, Phys. Rev. A **51**, 350 (1995).

[26] K. Wohrer, A. Chetioui, J. P. Rozet, A. Jolly, F. Fernandez, C. Stephan, B. Brendle, and R. Gayet, J. Phys. B **19**, 1997 (1986).
[27] L. Adoui, D. Vernhet, K. Wohrer, J. Plante, A. Chetioui, J. P. Rozet, I. Despiney, C. Stephan, A. Touati, J. M. Ramillion, A. Cassimi, J. P. Grandin, and M. Cornille, Nucl. Instrum. Methods Phys. Res. B **98**, 312 (1995).
[28] D. Vernhet, J. P. Rozet, K. Wohrer, L. Adoui, C. Stephan, A. Cassimi, and J. M. Ramillion, Nucl. Instrum. Methods Phys. Res. B **107**, 71 (1996).
[29] B. Brendle, R. Gayet, J. P. Rozet, and K. Wohrer, Phys. Rev. Lett. **54**, 2007 (1985).
[30] Th. Stöhlker, D. C. Ionescu, P. Rymuza, F. Bosch, H. Geissel, C. Kozhuharov, T. Ludziewjewski, P. H. Mokler, C. Scheidenberger, Z. Stachura, A. Warczak, and R. W. Dunford, Phys. Rev. A **57**, 845 (1998).
[31] Th. Stöhlker, D. C. Ionescu, P. Rymuza, F. Bosch, H. Geissel, C. Kozhuharov, T. Ludziejewski, P. H. Mokler, C. Scheidenberger, and Z. Stachura, Phys. Lett. A **238**, 43 (1998).
[32] D. C. Ionescu and Th. Stöhlker, Phys. Rev. A **67**, 022705 (2003).
[33] A. Gumberidze, Th. Stöhlker, G. Bednarz, F. Bosch, S. Fritzsche, S. Hagmann, D. C. Ionescu, O. Klepper, C. Kozhuharov, A. Krämer, D. Liesen, X. Ma, R. Mann, P. H. Mokler, D. Sierpowski, Z. Stachura, M. Steck, S. Toleikis, and A. Warczak, Hyperfine Interact. **146-147**, 133 (2003).
[34] K. Aashamar and P. A. Amundsen, J. Phys. B **14**, 483 (1981).
[35] P. A. Amundsen and K. Aashamar, J. Phys. B **14**, 4047 (1981).
[36] S. R. Valluri, U. Becker, N. Grün, and W. Scheid, J. Phys. B **17**, 4359 (1984).
[37] A. Surzhykov and S. Fritzsche, J. Phys. B **38**, 2711 (2005).
[38] N. Stolterfoht, R. D. DuBois, and R. D. Rivarola, *Electron Emission in Heavy Ion-Atom Collisions* (Springer, Berlin, 1997).
[39] A. B. Voitkiv, Phys. Rep. **392**, 191 (2004).
[40] A. B. Voitkiv, B. Najjari, and J. Ullrich, Phys. Rev. A **75**, 062716 (2007).
[41] D. A. Varshalovich, A. N. Moskalev, and V. K. Khersonkii, *Quantum Theory of Angular Momentum* (World Scientific, Singapore, 1988).
[42] E. G. Berezhko and N. M. Kabachnik, J. Phys. B **10**, 2467 (1977).
[43] K. Blum, *Density Matrix Theory and Applications* (Plenum, New York, 1981).
[44] I. P. Grant, Adv. Phys. **19**, 747 (1970).
[45] I. P. Grant, J. Phys. B **7**, 1458 (1974).
[46] G. Gaigalas, S. Fritzsche, and B. Fricke, Comput. Phys. Commun. **135**, 219 (2001).
[47] S. Fritzsche, Phys. Scr. **T100**, 37 (2002).
[48] S. Fritzsche, A. Surzhykov, and Th. Stöhlker, Phys. Rev. A **72**, 012704 (2005).
[49] F. A. Parpia, C. F. Fischer, and I. P. Grant, Comput. Phys. Commun. **94**, 249 (1996).
[50] S. Fritzsche, J. Electron Spectrosc. Relat. Phenom. **114-116**, 1155 (2001); S. Fritzsche, C. Froese Fischer, and G. Gaigalas, Comput. Phys. Commun. **148**, 103 (2002).
[51] Th. Stöhlker, D. C. Ionescu, P. Rymuza, F. Bosch, H. Geissel, C. Kozhuharov, T. Ludziewjewski, P. H. Mokler, C. Scheidenberger, Z. Stachura, A. Warczak, and R. W. Dunford, Phys. Rev. A **57**, 845 (1998).
[52] A. Gumberidze *et al.* (unpublished).